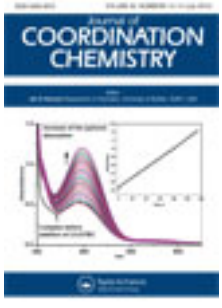

Journal of Coordination Chemistry
Publication details, including instructions for authors and subscription information:
http://www.tandfonline.com/loi/gcoo20

Structural characterization of two modifications of bis(4-methylpyridine)phthalocyaninato(2-)iron(II) complex

Jan Janczak [a] & Ryszard Kubiak [a]

[a] Institute of Low Temperature and Structure Research, Polish Academy of Sciences , Okólna 2 str. P.O. Box 1410, 50-950 Wrocław , Poland

Accepted author version posted online: 24 May 2012.Published online: 08 Jun 2012.

To cite this article: Jan Janczak & Ryszard Kubiak (2012) Structural characterization of two modifications of bis(4-methylpyridine)phthalocyaninato(2-)iron(II) complex, Journal of Coordination Chemistry, 65:14, 2478-2488, DOI: 10.1080/00958972.2012.696622

To link to this article: http://dx.doi.org/10.1080/00958972.2012.696622

Journal of Coordination Chemistry
Vol. 65, No. 14, 20 July 2012, 2478–2488

Structural characterization of two modifications of bis(4-methylpyridine)phthalocyaninato(2-)iron(II) complex

JAN JANCZAK* and RYSZARD KUBIAK

Institute of Low Temperature and Structure Research, Polish Academy of Sciences, Okólna 2 str. P.O. Box 1410, 50-950 Wrocław, Poland

(*Received 25 January 2012; in final form 24 April 2012*)

Two crystalline modifications, orthorhombic (**II**) and triclinic (**III**), of bis(4-methylpyridine) iron(II) phthalocyanine are obtained. The orthorhombic (**II**) crystals are formed from solvated crystals of FePc(4-Mepy)$_2 \cdot$ 2(4-Mepy) (**I**) after storing at room temperature in ambient air. The crystals **I** releasing the solvated 4-Mepy molecules transform into crystals **II** without destruction of the crystalline network. Releasing solvated 4-Mepy molecules from **I** and formation of **II** lead to co-operative translation of the neighboring zig-zag ribbons of FePc(4-Mepy)$_2$ and contraction of the lattice parameters. Triclinic crystals of FePc(4-Mepy)$_2$ (**III**) are formed at higher temperature than the orthorhombic, but solvated crystals of FePc(4-Mepy)$_2 \cdot$ 2(4-Mepy) (**I**). Electron paramagnetic resonance and magnetic susceptibility measurements clearly show ligation of the iron(II) phthalocyanine by 4-Mepy molecules leads to the change of the ground state from $S = 1$ (for FePc, $e_g^3 b_{2g}^2 a_{1g}^1$) to $S = 0$ (FePc(4-Mepy)$_2$, $e_g^4 b_{2g}^2$). Thus FePc(4-Mepy)$_2$ is a low-spin complex. The FePc(4-Mepy)$_2$ complex was also characterized by thermogravimetric analysis and UV-Vis spectroscopy.

Keywords: Iron phthalocyanine; 4 + 2 Coordinated FePc derivatives; Crystal structure; Transformation mechanism

1. Introduction

Iron(II) phthalocyanine belongs to the M(II)Pc colorant family known since the early years of the twentieth century [1, 2] and although studied for decades, still new FePc application perspectives are reported [3]. Iron phthalocyanine has very low solubility in most organic solvents and high tendency to aggregation that arises from strong π–π interactions between aromatic Pc-macrorings [4, 5]. FePc also exhibits a pronounced tendency to axial ligation with many additive FePc-complexes obtained by recrystallization of FePc from solvents with donors [6].

Thermal processing of FePc in ligating solvents like pyridine, picoline, and pyrazine allows one to obtain FePc-complexes, which possess tuned features in comparison to the parent FePc, which may be decisive for applications [7]. Among the ligating solvents pyridine and its derivatives are especially effective. With pyridine, FePc transforms into

*Corresponding author. Email: j.janczak@int.pan.wroc.pl

ISSN 0095-8972 print/ISSN 1029-0389 online © 2012 Taylor & Francis
http://dx.doi.org/10.1080/00958972.2012.696622

well developed and stable crystals of $FePc(py)_2$ [8]. However, as reported by Cariati *et al*. [9, 10], if FePc is thermally processed in 4-methylpyridine (4-Mepy) the formed $FePc(4\text{-}Mepy)_2$ complex co-crystallizes with solvent molecules forming well-developed crystals of $FePc(4\text{-}Mepy)_2 \cdot 2(4\text{-}Mepy)$ (**I**) containing two solvating 4-Mepy molecules in addition to the axially bonded 4-Mepy's. The latter crystals are far more susceptible to decomposition. Therefore from basic research as well as from the practical point of view the following question could be raised: In which conditions the colorant produced by recrystallization of FePc in 4-Mepy will be free of solvent?

2. Experimental

Iron(II) phthalocyanine (90%) and 4-methylpyridine (99%) were purchased from Aldrich-Sigma and used as received. Elemental analysis of the products was performed on an energy dispersive spectrometer. Thermal analyses were carried out on a Lineis L81 thermobalance apparatus with Pt crucibles; powdered Al_2O_3 has been used as a standard sample. The measurements were performed under static air on heating from room temperature to 350°C with heating rate of $5°C\,min^{-1}$. The sample left after thermogravimetric (TG) analysis was measured on a STOE diffractometer equipped with a linear PSD detector [11] using Cu-Kα_1 radiation ($\lambda = 1.54060$ Å) at room temperature. Electron paramagnetic resonance (EPR) measurements were carried out on SE-Radiopan and ESP 300 E-Bruker X-band spectrometers at room temperature. The studies were performed on solid samples of 5–10 mg. Temperature dependence of the magnetic susceptibility were studied from 1.8 K to 400 K with a Quantum Design SQUID magnetometer (San Diego, CA). Data were recorded at 0.5 T on samples of 50–80 mg. Measurements of electronic spectra were carried out at room temperature using a Varian-Cary 5E UV-Vis-NIR spectrometer. The spectra were recorded in dichloromethane solution (0.5 cm quartz cell) at room temperature. The concentration of the solution was $1 \times 10^{-5}\,mol\,L^{-1}$.

2.1. *Crystals of $FePc(4\text{-}Mepy)_2 \cdot 2(4\text{-}Mepy)$ (I), $FePc(4\text{-}Mepy)_2$ (II – orthorhombic phase) and $FePc(4\text{-}Mepy)_2$ (III – triclinic phase)*

Recrystallization of crude FePc in 4-Mepy was performed in a degassed sealed glass ampule as described previously [8]. Preliminary search by the X-ray diffraction of the fresh single crystals filtered from the mother liquor after one to several days prolonged thermal processing at 160°C or 120°C or even at 80°C show invariably the same crystalline lattice, consistent with that of $FePc(4\text{-}Mepy)_2 \cdot 2(4\text{-}Mepy)$ (**I**) [10]. Although, crystals of **I** at laboratory air at room temperature showed no visible change with prolonged storage small, but noticeable mass decay was observed. Therefore the crystals were inspected again after *ca* one year. The X-ray diffraction data confirmed their single crystalline form, but now the lattice parameters differ from that of $FePc(4\text{-}Mepy)_2 \cdot 2(4\text{-}Mepy)$ (**I**) [10]. Thus the crystals of **I** after about one year released the solvated 4-Mepy and transformed into orthorhombic $FePc(4\text{-}Mepy)_2$ crystals (**II**). Elemental analysis, found (%): Fe, 7.18; C, 70.31; N, 18.48; H, 4.03. Calculated for $C_{44}H_{30}N_{10}Fe$ (%): Fe, 7.40; C, 70.04; N, 18.56; H, 4.00.

When recrystallization of FePc (0.5 g) in 4-Mepy (10 mL) in sealed and degassed glass ampule was performed at 200°C during 2 days, the violet parallelepiped well-developed triclinic single crystals of FePc(4-Mepy)$_2$ (**III**) appeared. Elemental analysis, found (%): Fe, 7.29; C, 70.21; N, 18.48; H, 4.02. Calculated for $C_{44}H_{30}N_{10}Fe$ (%): Fe, 7.40; C, 70.04; N, 18.56; H, 4.00.

2.2. *Single-crystal X-ray data collection and structure determination*

Single crystals of **II** and **III** were used for data collection on a four-circle KUMA KM4 diffractometer equipped with 2-D CCD area detector. The graphite monochromated Mo-Kα radiation ($\lambda = 0.71073$ Å) and the ω-scan technique ($\Delta\omega = 1°$) were used for data collection. Data collection and reduction along with absorption corrections were performed using *CrysAlis* software [12]. The structure was solved by direct methods using *SHELXS-97* [13], which revealed positions of almost all non-hydrogen atoms. The remaining atoms were located from subsequent difference Fourier syntheses. The structure was refined using *SHELXL-97* [13] with anisotropic thermal displacement parameters. Hydrogen atoms were constrained: $U_{iso}(H) = 1.2U_{eq}$ of the aromatic carbons H with C–H distances of 0.93 Å and that of CH_3 with C–H distances of 0.96 Å.

Table 1. Crystallographic data and final refinement parameters for **II** and **III**.

	FePc(4-Mepy)$_2$	
	II	**III**
Empirical formula	$C_{44}H_{30}N_{10}Fe$	$C_{44}H_{30}N_{10}Fe$
Molecular weight	754.63	754.63
Temperature (K)	295(2)	295(2)
Crystal system	Orthorhombic	Triclinic
Space group	$P\,2_12_12_1$ (no. 19)[c]	P-1 (no. 2)
Unit cell dimensions (Å, °)		
a	10.110(2)	9.1710(18)
b	21.222(4)	9.981(2)
c	17.998(4)	10.950(2)
α		112.71(2)
β		91.06(1)
γ		110.41(1)
V (Å^3), Z	3861.6(13), 4	852.9(3), 1
θ range for data collection (°)	2.78–29.61	2.87–29.30
D_{calcd}/D_{exp} (g cm^{-1})	1.298/1.29	1.469/1.46
Absorption coefficient (mm^{-1})	0.436	0.494
Crystal size (mm^3)	$0.42 \times 0.25 \times 0.18$	$0.26 \times 0.24 \times 0.22$
T_{min}/T_{max}	0.8403/0.9288	0.8857/0.9015
Total/unique/Observed reflections	48,120/10,049/5143	11,114/4308/2924
R_{int}	0.0475	0.0348
R [$F^2 > 2\sigma(F^2)$][a]	0.0708	0.0389
wR [F^2 all reflections][b]	0.1580	0.0785
S	1.001	1.005
Flack parameter	0.12(5)	
Residual electron density, $\Delta\rho_{max}$, $\Delta\rho_{min}$ (e·Å^{-3})	0.482, −0.292	0.265, −0.420

[a] $R = \Sigma F_o - F_c/\Sigma F_o$.
[b] $wR = \{\Sigma\,[w(F_o^2 - F_c^2)^2]/\Sigma wF_o^4\}^{1/2}$; $w^{-1} = \sigma^2(F_o^2) + (aP)^2 + (bP)$, where $P = (F_o^2 + 2F_c^2)/3$. The a and b parameters are 0.0434 and 2.09 for **II**, 0.0320 and 0 for **III**.
[c] The non-standard setting of lattice parameter of **II** is selected for comparison with the lattice parameter of the crystal **I** ($a = 10.315(1)$, $b = 25.006(3)$ and $c = 17.876(2)$ Å [10]).

Table 2. Selected geometrical parameters for orthorhombic (**II**) and triclinic (**III**) crystals.

Orthorhombic FePc(4-Mepy)$_2$ (**II**)			
Fe–N1	1.889(3)	Fe–N3	1.974(4)
Fe–N5	1.900(4)	Fe–N7	1.903(4)
Fe–N9	2.057(4)	Fe–N10	2.004(4)
N1–Fe–N3	87.92(17)	N1–Fe–N5	178.0(2)
N1–Fe–N7	89.54(17)	N1–Fe–N9	90.40(16)
N1–Fe–N10	88.54(18)	N5–Fe–N3	90.09(17)
N5–Fe–N7	92.45(17)	N3–Fe–N7	177.45(17)
N5–Fe–N10	91.25(18)	N3–Fe–N10	89.68(18)
N7–Fe–N10	90.53(17)	N5–Fe–N9	89.75(15)
N3–Fe–N9	88.51(16)	N7–Fe–N9	91.22(18)
N10–Fe–N9	177.9(2)		
Triclinic FePc(4-Mepy)$_2$ (**III**)			
Fe–N1	1.9219(16)	Fe–N3	1.9344(14)
Fe–N5	2.0348(13)		
N1–Fe–N3	89.55(6)	N1–Fe–N3^{i}	90.45(6)
N1–Fe–N5	89.24(6)	N1–Fe–N5^{i}	90.76(6)
N3–Fe–N5	90.42(5)	N3–Fe–N5^{i}	89.58(5)
N1^{i}–Fe–N5^{i}	89.24(6)	N3^{i}–Fe–N5^{i}	90.42(5)
N1^{i}–Fe–N5	90.76(6)	N3^{i}–Fe–N5	89.58(5)

Symmetry code: (^{i}) $-x+1, -y, -z$.

Visualization of the structure was made with the Diamond 3.0 program [14]. Details of the data collection parameters, crystallographic data and final agreement parameters are listed in table 1. Selected geometrical parameters are listed in table 2.

3. Results and discussion

3.1. *Orthorhombic phase – II and the triclinic phase – III of FePc(4-Mepy)$_2$*

3.1.1. Thermal stability. TG analyses of solid samples of orthorhombic and triclinic modifications of FePc(4-Mepy)$_2$ are shown in figure 1. TG analysis shows that FePc(4-Mepy)$_2$ in both crystallographic modifications is stable to 220°C. Both modifications undergo decomposition at the same temperature (~220°C). Above this temperature FePc(4-Mepy)$_2$ loses ligated 4-Mepy from the Fe coordination environment and due to the high thermal motion of axial ligands the axial Fe–N bonds break simultaneously. The respective weight loss corresponds to the weight decrease by 24.67% due to release of two 4-Mepy from the complex. As can be seen from figure 1, the orthorhombic phase begins weight loss at 120°C. The orthorhombic FePc(4-Mepy)$_2$ (**II**) crystals are formed from solvated crystals of FePc(4-Mepy)$_2 \cdot 2$(4-Mepy) (**I**) after storing at room temperature in ambient air and therefore contain traces of solvating 4-Mepy responsible for the weight loss of ~1% (figure 1). There was no evidence of the formation of FePc(4-Mepy) – 1 : 1 adduct by thermal dissociation. Finally both modifications transform into β-FePc in powdered form that was confirmed by X-ray powder diffraction on a STOE powder diffractometer. The triclinic modifications of FePc(4-Mepy)$_2$ (**III**) in contrast to the orthorhombic FePc(4-Mepy)$_2 \cdot 2$(4-Mepy) (**I**) is stable at room temperature and in ambient air.

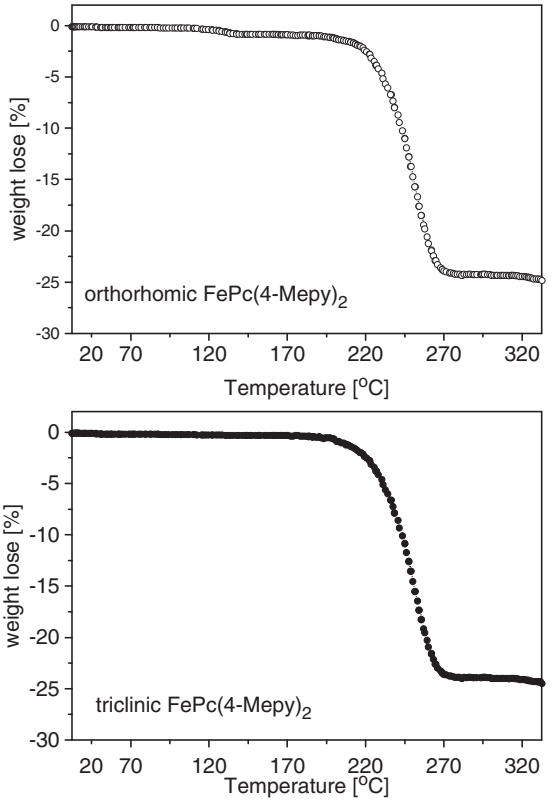

Figure 1. Thermograms of solid-state samples of orthorhombic and triclinic phases of $FePc(4\text{-}Mepy)_2$.

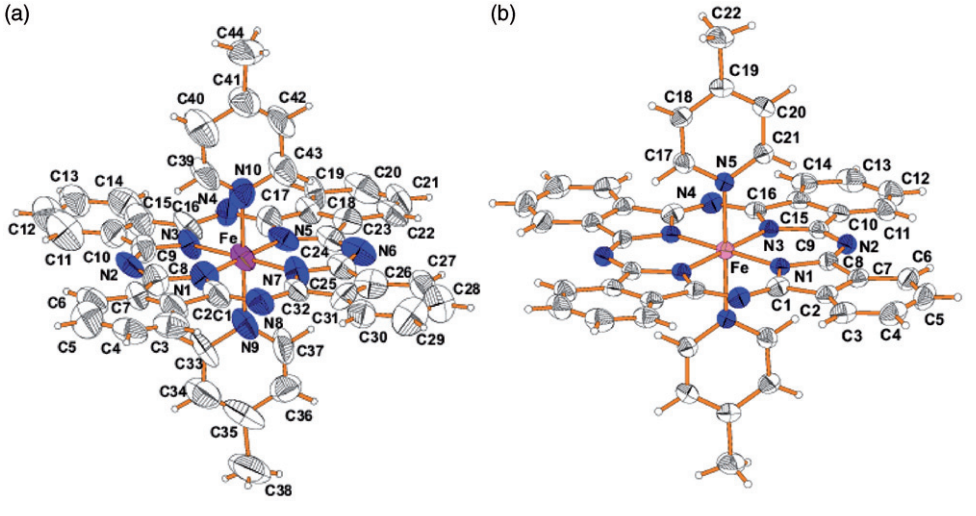

Figure 2. View of the orthorhombic (a) and triclinic (b) structures of $FePc(4\text{-}Mepy)_2$ showing the displacement ellipsoids at 50% probability.

3.1.2. Description of the orthorhombic phase – II and the triclinic phase – III of FePc(4-Mepy)$_2$ structures. The molecular structures of orthorhombic (**II**) and triclinic (**III**) FePc(4-Mepy)$_2$ are illustrated in figure 2(a) and (b). In both phases, the Fe(II) is equatorially coordinated by the four N-isoindoles of phthalocyaninato(2-) macrocycle and axially by 4-Mepy. The Fe(II) is $4+2$ coordinated in an approximate tetragonal bipyramid. In the triclinic modification Fe(II) lies at the inversion center, therefore the asymmetric unit consists of a half of FePc(4-Mepy)$_2$, while in the orthorhombic phase the whole FePc(4-Mepy)$_2$ molecule is asymmetric. The axial Fe–N bonds linking 4-Mepy are relatively strong but slightly longer (by ~0.1 Å) than the equatorial Fe–N bonds with Pc(2-) macrocycle (table 2). The axial and equatorial Fe–N bonds are quite similar in both **II** and **III**. The axial Fe–N bond lengths correlate well with the TG analyses. The dihedral angle between the N_4-isoindole plane of phthalocyaninato(2-) macrocycle and that containing the axially coordinated 4-Mepy in both phases is almost 90° (89.5(1)° and 89.7(1)° in **II** and **III**, respectively), but the orientation of two axial 4-Mepy molecules is slightly different in the two phases. Orientation of the axial 4-Mepy relative to the Pc(2-) macroring is well described by the torsion angle of N1–Fe–N9–C33 (in **II**) or by N1–Fe–C5–C21 (in **III**). Rotation of 4-Mepy around the axial Fe–N bond would reduce steric effect, i.e. the non-bonding distances between hydrogen atoms of 4-Mepy in ortho positions and the Pc(2-) macrocycle. In particular, if the rotation angle is 0, the ring plane of 4-Mepy ligand is parallel to the Fe–N1 bond, or at equivalent position rotated by 90°, the 4-Mepy ring plane is parallel to Fe–N3 bond, making the non-bonding C–H distances greater than 2.5 Å. The second orientation, with the rotation angle of 45°, makes the axial 4-Mepy ring plane parallel to the Fe–N(azamethine) axis and leads to interaction between ortho hydrogen atoms of 4-Mepy with the azamethine nitrogen atoms of Pc(2-). These N···H interactions stabilize the orientation of the axial 4-Mepy ligands and the conformation of FePc(4-Mepy)$_2$. This conformation of FePc(4-Mepy)$_2$ is preferable in solution. The intermolecular interactions as well as the crystal packing forces present in the crystals make the rotation of the axial 4-Mepy ring plane 43.9(2)° in the orthorhombic phase and 38.1(1)° in the triclinic phase. These angles are slightly different from that observed in the axially ligated pyridine iron phthalocyanine complex, FePc(py)$_2$ [8] as well as in the solvated complex FePc(4-Mepy)$_2 \cdot 2$(4-Mepy) (**I**) [10] (table 3).

The arrangement of FePc(4-Mepy)$_2$ molecules in crystals **II** and **III** is mainly determined by van der Waals forces. FePc(4-Mepy)$_2$ is relatively large and extends in the Pc plane and the 4-Mepy biaxially coordinated molecules act as a steric hindrance. Since crystals **II** are formed from **I** after storing at room temperature in ambient air, therefore molecular arrangement of FePc(4-Mepy)$_2$ in **II** will be compared with that in **I**.

Table 3. Comparison of the Fe(II) coordination in 4+2 coordinated FePc-complexes.

Compound	Average equatorial Fe–N_{iso} (Å)	Axial Fe–N (Å)	Rotation angle of axial ligand (°)	Ref.
FePc(4-Mepy)$_2$ – triclinic	1.928(2)	2.035(2)	38.1(1)	This work
FePc(4-Mepy)$_2$ – orthorhombic	1.915(4)	2.030(4)	43.9(2)	This work
FePc(4-Mepy)$_2$·2(4-Mepy) (**I**)	1.935(3)	2.040(3)	42.6(4)	[10]
FePc(py)$_2$	1.938(2)	2.039(2)	36.1(2)	[8]

FePc(4-Mepy)$_2$ in **I** are arranged in zig-zag ribbons along the *c*-direction. Such arrangement of large FePc(4-Mepy)$_2$ left voids in the crystalline network that are occupied by 4-Mepy, as shown in figure 3(a). When **I** is stored at ambient air at room temperature during 1 year, crystals **I** transform to **II**, releasing solvated 4-Mepy. This transformation takes place without destruction of the crystals, since releasing of 4-Mepy from crystals of **I** is very slow. The collective thermal motions of the zig-zag ribbons of FePc(4-Mepy)$_2$ as anchors are the causes of the displacement slowly releasing 4-Mepy from the crystal **I** and finally the frame network consists of only FePc(4-Mepy)$_2$. The transformation of crystals of **I** with releasing of 4-Mepy into crystals of **II** results in contraction of the cell volume of 4610.9(3) Å^3 to 3861.6(13) Å^3. Contraction of the lattice parameters of the unit cell is clearly evidenced in the longest lattice parameter, $b = 25.006(3)$ Å in **I** decrease to $b = 21.222(4)$ Å in **II**, the other two lattice parameters (*a* and *c*) are practically unchanged, since the dihedral angle between the Pc ring planes of neighboring molecules are almost the same in both **I** and **II**. Releasing 4-Mepy from crystals of **I** leads to cooperative and in the opposite direction translation of the neighboring zig-zag ribbons of FePc(4-Mepy)$_2$ molecules by $\pm 1/8$ along the [001] direction (figure 3). These opposite shifts of the neighboring zig-zag ribbons result in contraction of the lattice parameters, filling of the voids left after releasing 4-Mepy, and yield crystals of **II** (figure 3b). However, the filling of the space in **II** is worse than in **I**, also reflected in the respective crystal densities: $d = 1.355\ \mathrm{g\,cm^{-3}}$ in **I** and $d = 1.298\ \mathrm{g\,cm^{-3}}$ in **II**. The less packed FePc(4-Mepy)$_2$ molecules in **II** than in **I** is also evidenced by the relatively great anisotropic thermal motions. The anisotropic displacement ellipsoids, shown in figure 1 (at the 50% probability level), for FePc(4-Mepy)$_2$ are twice bigger in **II** than in **III**.

The arrangement of FePc(4-Mepy)$_2$ in the triclinic crystal **III**, in contrast to **I** and **II** in which the molecules form alternating zig-zag ribbons along the *c*-direction with the

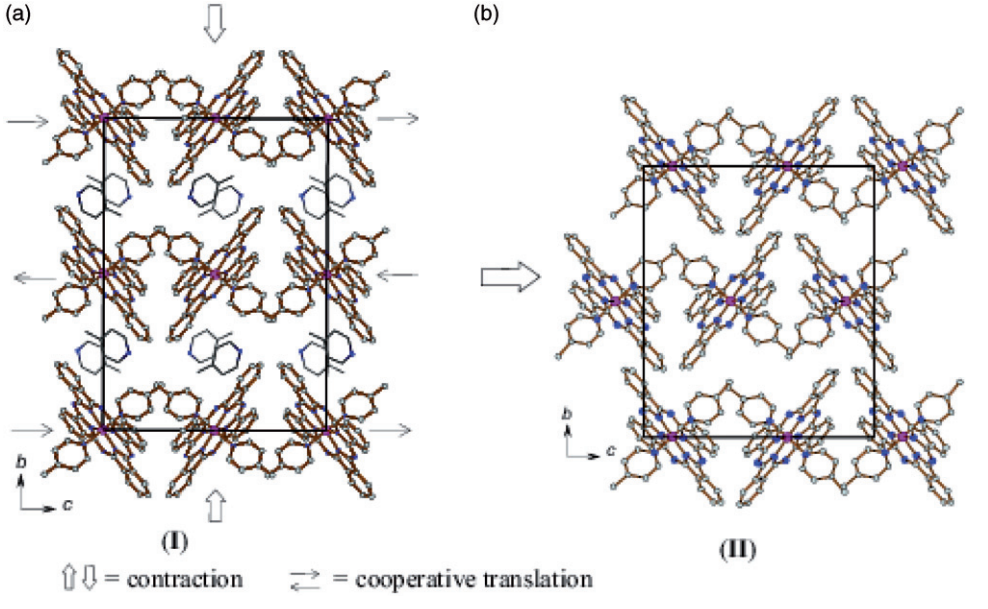

Figure 3. View of the crystal packing of (**I**), (a), and (**II**), (b), showing the cooperative translation of zig-zag chains of FePc(4-Mepy)$_2$ and contraction of the lattice parameters.

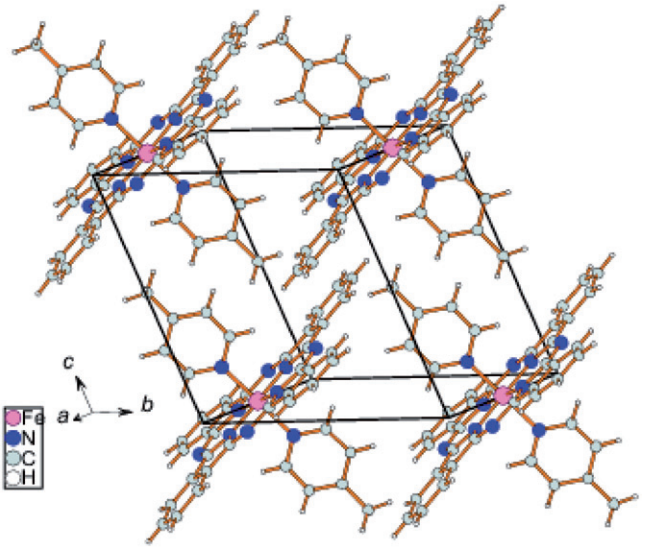

Figure 4. The crystal packing of triclinic phase of FePc(4-Mepy)$_2$.

dihedral angle between the Pc ring plans of ~89°, are almost parallel, i.e. the Pc ring planes are parallel (figure 4). This parallel arrangement of FePc(4-Mepy)$_2$ in **III** is reflected in the crystal densities (1.469 g cm^{-3} – **III**, 1.355 g cm^{-3} – **I** and 1.298 g cm^{-3} – **II**). However, due to the steric hindrance of the biaxially coordinated 4-Mepy molecules to the Fe center of FePc, the molecular arrangement of FePc(4-Mepy)$_2$ is not stabilized by π–π interactions between the aromatic Pc(2-) macrorings of FePc(4-Mepy)$_2$ molecules as is observed in the parent FePc structure [15].

3.1.3. Magnetic properties. The magnetic susceptibility of the parent iron phthalocyanine, FePc, has been performed several times [16–19] and the effective magnetic moment is intermediate between the theoretical spin-only values for $S=1$ and $S=2$ states. Mössbauer studies on the FePc [20–22] indicate that the central Fe in FePc is in $S=1$ state with a large zero-field splitting such that the level $M_S=0$ lies about 70 cm^{-1} below the doublet $M_S=\pm1$ [20]. The electronic configuration was assumed to be $(d_{xz}d_{yz})^3(d_{xy})^2(d_z^2)^1$ giving an orbitally non-degenerate ground term $^3B_{2g}$ with two unpaired electrons. EPR measurements performed on solid polycrystalline orthorhombic (**II**) and triclinic (**III**) phases of FePc(4-Mepy)$_2$ showed no resonance signal. The magnetic susceptibility experiments on solid **II** and **III** show diamagnetic character. Thus both experiments show that upon ligation of the iron(II) phthalocyanine by 4-Mepy with formation of biaxially coordinated FePc(4-Mepy)$_2$ leads to the change of the ground state from $S=1$ (for FePc, $e_g^3b_{2g}^2a_{1g}^1$) to $S=0$ (for FePc(4-Mepy)$_2$, $e_g^4b_{2g}^2$). Thus FePc(4-Mepy)$_2$ is a low-spin complex, according to the molecular orbital diagram of Fe(II) in a strong-field tetragonal environment [23].

3.1.4. UV-Vis spectroscopy. Electronic absorption spectra of FePc(4-Mepy)$_2$ and FePc in dichloromethane solutions, for comparison, are shown in figure 5. The UV-Vis spectrum of FePc(4-Mepy)$_2$ in CH_2Cl_2 solution, similar to the spectrum of FePc, shows

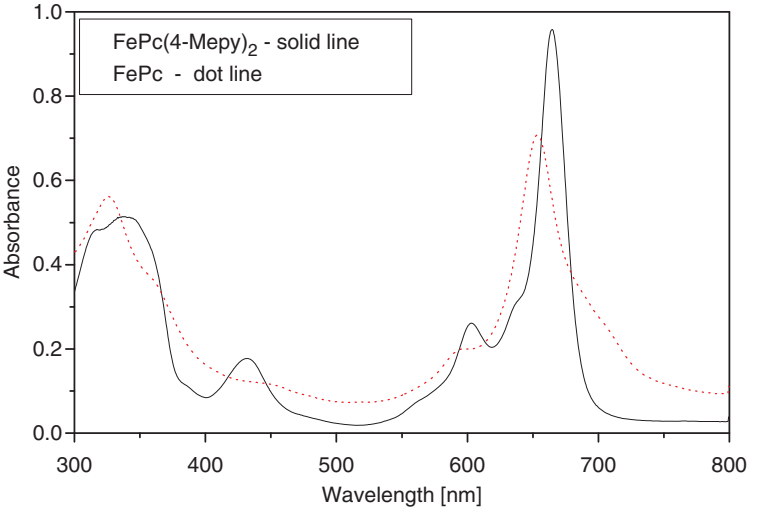

Figure 5. UV-Vis spectrum of FePc(4-Mepy)$_2$ (—) and FePc (···) in dichloromethane.

two bands (Q and B) characteristic for the phthalocyaninato(2-) macrocycle [24]. In the spectrum of FePc(4-Mepy)$_2$, the Q band is observed at 665 nm ($\log \varepsilon = 4.87$) and the B band at ~340 nm ($\log \varepsilon = 4.61$). The Q band corresponds to excitation between the HOMO (a_{1u}) to LUMO (e_g), while the B band corresponds to HOMO-1 (a_{2u}) to LUMO (e_g) transition. The respective bands in the spectrum of the parent FePc in CH_2Cl_2 solution are at 655 nm (Q) and ~330 nm (B). Thus the Q and B bands in FePc(4-Mepy)$_2$ are red shifted by ~10 nm compared to that in FePc. As can be seen from figure 5, the Q band in the spectrum of FePc(4-Mepy)$_2$ as well as FePc splits into two bands. The splitting value is ~60 nm due to vibronic coupling in the excited state [25–27]. The spectrum of FePc(4-Mepy)$_2$ shows one additional band at ~430 nm ($\log \varepsilon = 3.13$) compared to the spectrum of the parent FePc. Several authors have assigned the band at 430 nm to the electronic transition from a deeper level to the half-occupied HOMO level. Thus, the band is an evidence for existence of the one-electron oxidized free radical phthalocyaninato(1-$^{\cdot}$) macroring as observed in the spectrum of one-electron oxidized metallophthalocyaninato and diphthalocyaninato complexes, such as lithium phthalocyanine (LiPc), lanthanide diphthalocyanine (Ln(III)Pc$_2$), and indium diphthalocyanine (InPc$_2$) [28–33]. However, the EPR experiment on the solid state sample of FePc(4-Mepy)$_2$ showed no signal, therefore the observed band at 430 nm cannot be attributed to the transition in the radical form of Pc(1-$^{\cdot}$), since the magnetic measurements show $FeCl_2(pyz)_2$ is a low-spin complex ($S = 0$, ground state of $e_g^4 t_{2g}^2$) and does not possess a hole in the e_g level. Kobayashi and Yanagawa [34] studied the dipyridine iron(II) tetraphenyl porphyrin assigning the band at 21,000 cm^{-1} (~415 nm) to charge transfer from iron to axially coordinated pyridine, $b_{2g}(d_\pi) \rightarrow b_{3u}(2p_z^*)$. This assignment seems reasonable. Thus the additional band at 430 nm in the spectrum of FePc(4-Mepy)$_2$ should be attributed to charge transfer from iron to axially ligated 4-Mepy, since a similar additional band has also been observed in the spectrum of FePc(py)$_2$ [8].

4. Conclusion

The synthesis of FePc(4-Mepy)$_2$ at temperature below 180°C yields the solvated FePc(4-Mepy)$_2 \cdot 2$(4-Mepy) crystals (**I**), which are moderately stable at room temperature in ambient atmosphere. The orthorhombic crystals of **I** with prolonged storage lose solvated 4-Mepy and transform into FePc(4-Mepy)$_2$ orthorhombic crystals (**II**). To obtain the stable solid-state FePc(4-Mepy)$_2$ (**III**) the synthesis must be performed at higher temperature (~200°C).

Supplementary material

Details on data collection and refinement, fractional atomic coordinates, anisotropic displacement parameters, and full list of bond lengths and angles in CIF format have been deposited with the Cambridge Crystallographic Data Centre, Nos CCDC 863783 and 863784. Copies of this information can be obtained free of charge from The Director, CCDC, 12 Union Road, Cambridge, CB2 1EZ, UK (Fax: +44-1223-336-033; E-mail: deposit@ccdc.cam.ac.uk or www: http://www.ccdc.cam.ac.uk).

References

[1] R.P. Linstead, J.M. Robertson. *J. Chem. Soc.*, 1736 (1937).
[2] J.M. Robertson. *Organic Crystals and Molecules*, p. 263, Cornell University Press, Ithaca, NY (1953).
[3] (a) C. Isvoranu, B. Wang, K. Schulte, E. Ataman, J. Knudsen, J.N. Andersen, M.L. Bocquet, J. Schnadt. *J. Phys.: Condens. Matter*, **22**, 472002 (2010); (b) H.G. Zhang, J.T. Sun, T. Low, L.Z. Zhang, Y. Pan, Q. Liu, J.H. Mao, H.T. Zhou, H.M. Guo, S.X. Du, F. Guinea, H.J. Gao. *Phys. Rev. B*, **84**, 245436 (2011); (c) L.X. Alvarez, E.V. Kudrik, A.B. Sorokin. *Chem. Eur. J.*, **17**, 9298 (2011); (d) Z.H. Cheng, L. Gao, Z.T. Deng, Q. Liu, N. Jiang, X. Lin, X.B. He, S.X. Du, H.J. Gao. *J. Phys. Chem. C*, **111**, 2656 (2007); (e) S. Liu, X. Jiang, G. Zhuo. *New J. Chem.*, **31**, 916 (2007); (f) C. Isvoranu, B. Wang, E. Ataman, K. Schulte, J. Kundsen, J.N. Andersen, M.L. Bocquet, J. Schnadt. *J. Chem. Phys.*, **134**, 114710 (2011).
[4] J. Obiari, N.P. Rodrigues, F. Bedioui, T. Nyokong. *J. Porphyrins Phthalocyanines*, **7**, 508 (2003).
[5] D.S. Terekhov, K.J.M. Nolan, C.R. McArthur, C.C. Leznoff. *J. Org. Chem.*, **61**, 3034 (1996).
[6] V.N. Nemynkin, I.N. Tretyakova, S.V. Volkov, V.D. Li, N.G. Mekhryakova, O.L. Kaliya, E.A. Lukyantes. *Russ. Chem. Rev.*, **69**, 325 (2000).
[7] J. Janczak, R. Kubiak. *CrystEngComm*, **12**, 3599 (2010).
[8] J. Janczak, R. Kubiak. *Inorg. Chim. Acta*, **342**, 64 (2003).
[9] F. Cariati, D. Gallizoli, F. Morazzoni. *J. Chem. Soc., Dalton Trans.*, 556 (1975).
[10] F. Cariati, F. Morazzoni, M. Zocchi. *J. Chem. Soc., Dalton Trans.*, 1018 (1978).
[11] *WinXPow Software Manual*, STOE & GmbH, Darmstadt, Germany (1997).
[12] *CrysAlis CCD and CrysAlis Red program, Ver. 171.31.8*, Oxford Diffraction Poland, Wrocław, Poland (2006).
[13] G.M. Sheldrick. *SHELXS97*, *SHELXL97*, *Programs for Crystal Structure Solution and Refinement*, University of Göttingen, Göttingen, Germany (1997).
[14] K. Brandenburg, K. Putz, *Diamond, Ver. 3.0*, *Crystal and Molecular Structure Visualization*, University of Bonn, Germany (2006).
[15] J.F. Kirner, W. Dow, W.R. Scheidt. *Inorg. Chem.*, **15**, 1685 (1976).
[16] A.B.P. Lever. *J. Chem. Soc. (London)*, 1821 (1965).
[17] R.L. Martin, S. Mitra. *Chem. Phys. Lett.*, **3**, 183 (1969).
[18] B.W. Dale, R.J.P. Williams, T.L. Thorp. *J. Chem. Phys.*, **49**, 3441 (1965).
[19] C.G. Barrsclough, R.L. Martin, S. Mitra, R.C. Sherwood. *J. Chem. Phys.*, **53**, 1643 (1970).
[20] B.W. Dale, R.J.P. Williams, R.P. Edwards, C.E. Johnson. *J. Chem. Phys.*, **49**, 3445 (1965).
[21] A. Hudson, H.J. Whitefield. *Inorg. Chem.*, **6**, 1120 (1967).
[22] T.H. Moss, A.B. Robinson. *Inorg. Chem.*, **7**, 1692 (1968).

[23] B.W. Dale, A.B. Williams, R.P. Edwards, C.E. Johnson. *Trans. Faraday Soc.*, **64**, 620 (1968).
[24] L. Edwards, M. Gouterman. *J. Mol. Spectrosc.*, **33**, 292 (1970).
[25] T. Nozawa, N. Kobayashi, H. Hatamo, M. Ueda, M. Sogami. *Biochim. Biophys. Acta*, **626**, 282 (1980).
[26] T. Nykong, Z. Gasyna, M.J. Stillman. *Inorg. Chem.*, **26**, 1087 (1987).
[27] T.C. VanCott, J.L. Rose, G.M. Meisener, B.E. Williamson, A.E. Schrimp, M.E. Boyle, P.N. Schatz. *J. Phys. Chem.*, **93**, 2999 (1989).
[28] J. Janczak. *Pol. J. Chem.*, **72**, 1871 (1998).
[29] P. Turek, J.J. Andre, J. Giraudeau, J. Simon. *Chem. Phys. Lett.*, **134**, 471 (1987).
[30] H. Homborg, W. Kaltz. *Z. Naturf. Teil B*, **33**, 1067 (1978).
[31] E. Ort, J.E. Bredas, C. Clarise. *J. Chem. Phys.*, **92**, 1228 (1990).
[32] H. Sugimoto, T. Higashi, M. Mori. *J. Chem. Soc., Chem. Commun.*, 622 (1983).
[33] H. Sugimoto, T. Higashi, M. Mori. *Chem. Lett.*, **12**, 1167 (1983).
[34] T. Kobayashi, Y. Yanagawa. *Bull. Chem. Soc. Japan*, **45**, 450 (1972).